

Peer Reviewed Paper **openaccess** [Paper Presented at HSI 2014, Coventry, UK](#)

# Hyperspectral analysis for extraction of chemical characteristics in dehydrated bones

Carolina Blanch-Perez-del-Notario\* and Andy Lambrechts

Imecc, Kapeldreef 75, 3001, Leuven, Belgium. E-mail: Carolina.Blanch@imecc.be

Gelatin, a valuable commodity in food processing, pharmaceuticals and photography, is produced by boiling the connective tissues, bones and skins of animals. To be able to predict the quality of the resulting gelatin, a number of parameters, such as percentage of fat, protein, water and mineral content, are measured in the raw bones. We evaluate in this paper whether hyperspectral imaging can perform the required fast and accurate prediction of these parameters based on the spectral response of bone samples. This would allow replacing the time-consuming chemical analysis. The spectral response of nine different bone batches in the 600–1000 nm range (Vis-NIR) is correlated by means of Partial Least Square regression with the measured parameters. Our results show that high prediction accuracy can be obtained for all measured parameters based on the Vis-NIR spectral response. We can then conclude that hyperspectral imaging is a promising metric for the estimation of these chemical characteristics.

**Keywords:** Vis-NIR spectral response, chemical characteristics, regression

## Introduction

Gelatin is a protein substance derived from collagen, a natural protein present in skin, bones and animal tissue. Its ability to form strong, transparent gels and flexible films has made it a valuable commodity in food processing, paper production, photography and pharmaceuticals. When used for pharmaceutical purposes, gelatin is recovered from bone. In its manufacturing process a number of steps are taken, such as chopping the bones, degreasing them to reduce the fat content and dehydrating them in industrial dryers. Next, an acid/alkaline treatment is followed by soaking the bones for approximately five days. This process removes most of the minerals and bacteria and facilitates the release of collagen. Finally, the pieces of bone are boiled in distilled water and the liquid that now contains gelatin can be drawn off.

To be able to predict the quality of the resulting gelatin, a number of characteristics need to be known from the raw sample bones, such as percentages of fat, protein, water and mineral content. Generally, a chemical analysis is performed on the degreased and dehydrated bones to extract this information. Ideally, we would like to know the characteristics of the sample batch to be able to discard it before proceeding to the acid/alkaline treatment. However, current chemical analysis cannot be performed in a timely manner and the acid treatment is started before the bone characteristics and quality level are known. Moreover, due to efficiency constraints, the analysis is only performed on a small subset of the batch. For a more efficient use of resources, a faster and robust evaluation technique of these bone properties is desired. This would allow the screening of larger numbers of bone samples while rapidly

### Correspondence

C. Blanch-Perez-del-Notario ([Carolina.Blanch@imecc.be](mailto:Carolina.Blanch@imecc.be))

**Received:** 30 April 2015

**Revised:** 7 April 2017

**Accepted:** 7 September 2017

**Publication:** 22 September 2017

**doi:** 10.1255/jsi.2017.a5

**ISSN:** 2040-4565

### Citation

C. Blanch-Perez-del-Notario and A. Lambrechts, "Hyperspectral analysis for extraction of chemical characteristics in dehydrated bones", *J. Spectral Imaging* 6, a5 (2017). <https://doi.org/10.1255/jsi.2017.a5>

© 2017 The Authors

This licence permits you to use, share, copy and redistribute the paper in any medium or any format provided that a full citation to the original paper in this journal is given, the use is not for commercial purposes and the paper is not changed in any way.



extracting the required information before the bones undergo any further time-consuming process.

For this purpose, we evaluate the suitability of hyperspectral imaging to perform the required fast and accurate prediction of these parameters (water, fat, protein and mineral content) based on the spectral response of dehydrated bone samples. Similar studies in literature have focused on extracting chemical characteristics by means of hyperspectral imaging. This way, in Reference 1, Vis/NIR spectral analysis together with regression techniques showed to be an accurate method for pH value prediction in salmon fillets. Similarly, in Reference 2, analysis of Vis/NIR spectra also proved to be an efficient method for prediction of moisture and fat content of fried breaded chicken nuggets. Finally, in Reference 3, the authors used NIR hyperspectral imaging to analyse the presence of collagen in bones from archaeological sites, although no estimation of specific collagen percentages was extracted.

## Materials and methods

We use a proprietary Imec line scan sensor<sup>4</sup> to acquire the bone spectral responses in the 600–1000nm range (Vis-NIR). Our novel hyperspectral sensor integrates a wedge filter on top of a standard CMOS sensor resulting in a compact and fast hyperspectral sensor of 4 megapixels. Our sensor acquires 100 spectral bands over a spectral range from 600nm to 1000nm, with a spectral resolution better than 10nm and a spatial resolution of 2048pixels per line. We use it to measure the spectral response of nine different batches of dehydrated bones for which a chemical analysis has already been provided for, as given in Table 1. We compare and correlate the spectral response with the measured percentages of humidity, fat, proteins and minerals by means of Partial Least Squares (PLS) regression. Prior to this, some

preprocessing, such as outlier removal and SNV normalisation, is applied to reduce the inherent spectral variability within the samples. The regression model obtained is then cross-validated with calibration and validation sets. The preprocessing can be detailed as follows:

- The **outlier removal procedure** aims at eliminating image pixels corresponding to background, cracks or specular reflections that should not be considered for the computation of the mean bone spectra. To do so, we compute the mean and standard deviation of the set of batch samples. Any point whose Euclidean distance to the mean of the set is higher than three times the standard deviation is considered an outlier or non-representative sample. After all outliers have been removed, the new mean and standard deviation are computed. This process runs iteratively until no more outliers can be found.
- **Standard Normal Variate (SNV)**: corrects the light scattering and reduces the inherent spectral variability within the samples. This normalisation calculates the standard deviation of all the pooled variables for the given sample. The entire sample is then normalised by this value, thus giving the sample a unit standard deviation. It performs as well spectral detrending by subtracting the individual mean value from each spectrum.
- **Spectral averaging**: the amount of bone samples provided allows us to scan five petri dishes per batch type. We take approximately 100,000 bone pixels per petri dish image, building a total of 500,000 samples. After outlier removal and SNV normalisation, we obtain 10 sets of mean spectral signatures, thus each spectral mean corresponds roughly to the number of samples in half a petri dish. Computing these averages is required to deal with the strong spectral variation present in the image. These mean spectra are then fed into the regression model together with the corresponding chemically measured percentages shown in Table 1.

**Table 1. Measured properties for bone samples.**

	Batch #1	Batch #2	Batch #3	Batch #4	Batch #5	Batch #6	Batch #7	Batch #8	Batch #9
Humidity	9.29%	10.26%	11.59%	8.54%	11.40%	10.19%	10.20%	9.65%	8.32%
Fat	2.05%	2.08%	2.26%	2.09%	4.97%	2.27%	2.74%	2.90%	2.41%
Protein	28.78%	30.43%	31.83%	28.59%	29.58%	30.52%	30.88%	35.31%	25.65%
Mineral	58.35%	58.54%	54.85%	59.90%	51.23%	54.21%	54.21%	49.81%	59.03%

Regarding Table 1, note that the sum of the different components should amount to 100%, but in reality it ranges between 98% and 101%. This is due to limitations in the chemical analysis accuracy and slight differences in samples collected for each measurement. The impact of these inaccuracies in the chemical measurement is that we are feeding the regression model with slightly inaccurate output values, which could degrade the model performance. Ideally, more accurate chemical analysis should be performed to optimise the training of the model.

For the training and testing of the model we try two different approaches. In the first approach we build the regression model with a calibration set of five mean spectra per batch and a validation set of the remaining five mean spectra. We choose to do since we consider that the bone batches are quite heterogeneous between and within batches, so we wish to require the training of the model with as many batches as possible.

On the other hand, to avoid potential overfitting of the model we try a second approach in which one bone batch is left out of the training at a time and considered as a test batch. This way, we use the 10 mean spectra of 8 batches for calibrating the model while we use the remaining batch for testing. The training and testing batches are rotated and all combinations tested. The results for both approaches are discussed in next section.

## Results and discussion

We first present the results of our first approach. Figures 1–4 show the regression predicted contents for each of the validation samples versus the chemically measured contents. The cross-validated coefficient of determination ( $R^2_{cv}$ ) and root mean square error of cross-validation (RMSECV) are provided as well. The choice for the number of PLS components to be used is made after comparing the resulting  $R^2_{cv}$  coefficient obtained for a range of number of PLS components used in the model. The best results are obtained for around seven to eight PLS components, therefore used to generate the graphs in this paper (seven components for moisture and protein prediction and eight for fat and mineral prediction).

We can observe that high prediction accuracy is achieved for all measured parameters with a slightly lower accuracy for fat content prediction.

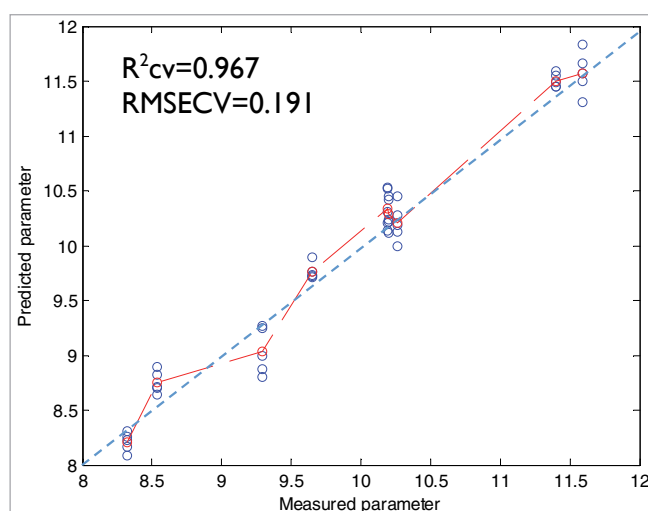


Figure 1. Measured and predicted humidity content (%).

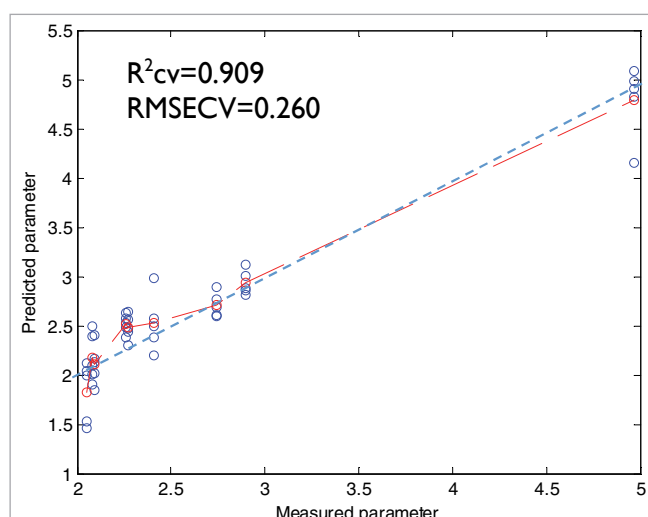


Figure 2. Measured and predicted fat content (%).

In Figures 1–4 the average prediction value of the test set considered is connected by the dashed lines, lying closely to the line where the measured parameter equals the predicted one. We can obtain a more accurate estimation of chemical characteristics by averaging over several prediction sets. This way, we perform  $5 \times 5$  cross-validation in 10 different random distributions of training and testing sets. By averaging then the predicted values over the test samples in the 10 training-test distributions, we obtain more accurate estimations, as shown by the reduction in the root mean square error (RMSE) of the average prediction in Table 2. This indicates that analysing a wider sample set can potentially increase the prediction accuracy.

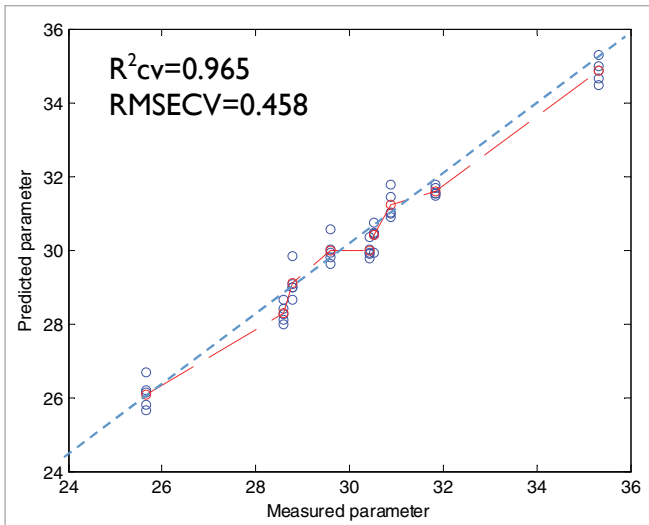


Figure 3. Measured and predicted protein content (%).

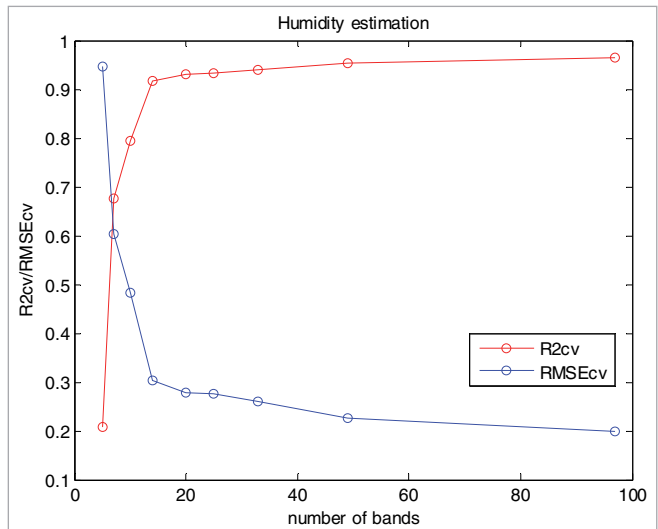


Figure 5. Accuracy versus bands for humidity estimation.

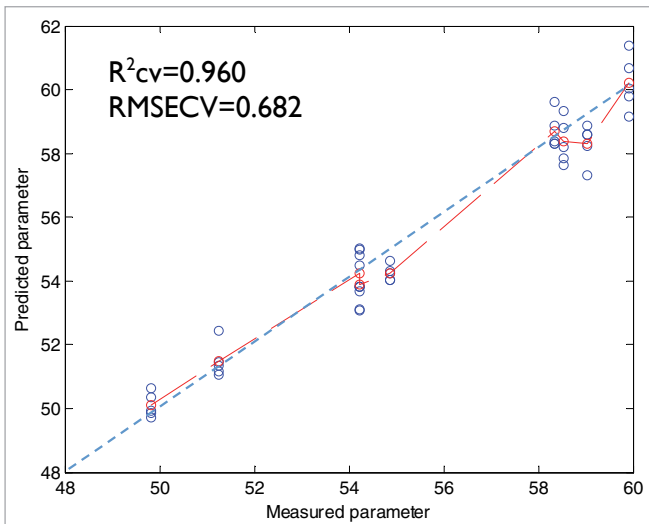


Figure 4. Measured and predicted mineral content (%).

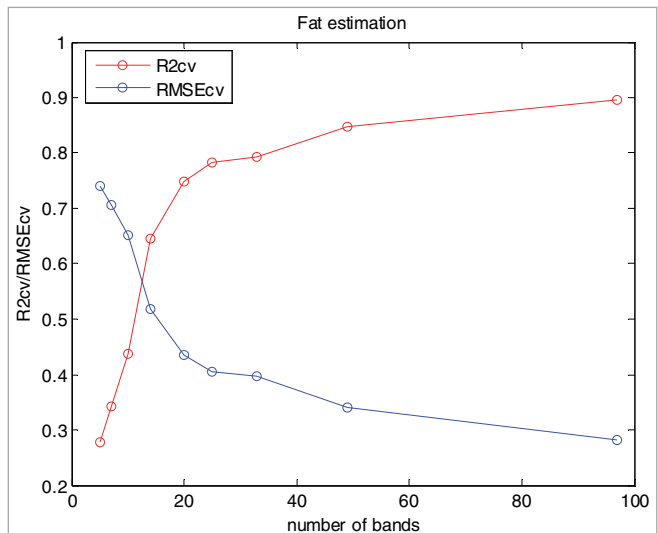


Figure 6. Accuracy versus bands for fat estimation.

In Table 2, we also indicate the percentile of the error on the average value of a specific parameter. This expresses, for instance, how an error of absolute value around 0.2 corresponds to a higher percentile error for fat prediction than for humidity prediction.

On top of this we have analysed the impact of the number of bands considered on the model accuracy obtained. Figures 5 and 6 show the corresponding  $R^2_{cv}$  and  $RMSECV$  values for a choice of bands decreasing from 98 to 5 bands and the prediction of humidity and fat, respectively.

Table 2. RMSE decrease by averaging over predictions.

	Humidity	Fat	Protein	Mineral
$RMSECV$	0.191 (1.99%)	0.260 (9.84%)	0.458 (1.51%)	0.682 (1.22%)
$RMSE$ mean prediction	0.0185 (0.18%)	0.101 (3.8%)	0.355 (1.17%)	0.267 (0.5%)

Table 3. Model accuracy versus number of bands considered.

$R_{cv}^2$ / $RSME_{cv}$	Humidity	Fat	Protein	Mineral
98 bands	0.96/0.19	0.89/0.28	0.96/0.45	0.95/0.73
49 bands	0.95/0.22	0.84/0.34	0.95/0.49	0.92/0.91
33 bands	0.94/0.26	0.79/0.39	0.95/0.54	0.91/1.0
25 bands	0.93/0.27	0.78/0.40	0.93/0.66	0.83/1.37
20 bands	0.93/0.28	0.74/0.43	0.93/0.63	0.83/1.37
14 bands	0.9/0.301	0.64/0.51	0.92/0.66	0.79/1.52
10 bands	0.79/0.48	0.43/0.65	0.90/0.77	0.64/2.02
7 bands	0.67/0.60	0.34/0.70	0.87/0.88	0.66/2.02
5 bands	0.20/0.94	0.27/0.73	0.73/1.26	0.43/2.55

To do so we first extract with the Variable Importance Projection technique<sup>5,6</sup> the relative weight per wavelength and use these relevance ratings to pick the most relevant bands, for each number of bands considered. We can see in Figure 5 that with 14 bands we already achieve high prediction accuracy ( $R_{cv}^2$  of 0.9) for humidity estimation. As also shown in Table 3, for fat and mineral estimation we need 33 bands for high accuracy while for humidity and protein estimation 14 bands seem to suffice.

The results of the second approach for model calibration and validation is reported next. Figure 7 shows the predicted versus measured humidity when training the model with batches 2–9 (blue) and testing it on batch 1 (red). Figure 8 shows similar estimation when the model is trained with all batches except batch number 3 (red)

and this is used as test batch. In this case, we can see that some underestimation happens, probably since this batch is at one of the extremes of the range considered.

This process is repeated for all parameter estimation and for all batches taken consecutively as test batch out of the training set. Table 4 summarises these results showing the average percentile error made in the parameter prediction per test batch. Out of the nine available batches, eight are taken for training the model and the remaining one is used to test the model. From the results, we can see that the estimation of humidity, protein and mineral content on out-of-training test batches provides reasonable accuracy. On batches 5–7 the error tends to be a bit higher while on the remaining batches the mean error incurred is of 5% for humidity and mineral and of 8% for protein estimation.

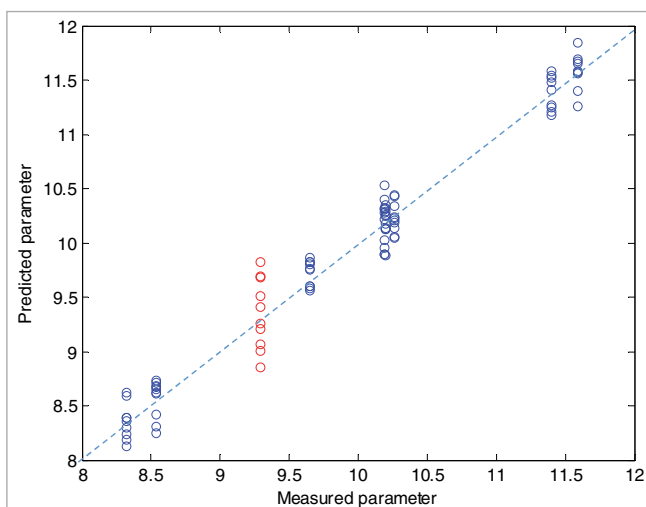


Figure 7. Humidity estimation for out-of-training set bone Batch #1.

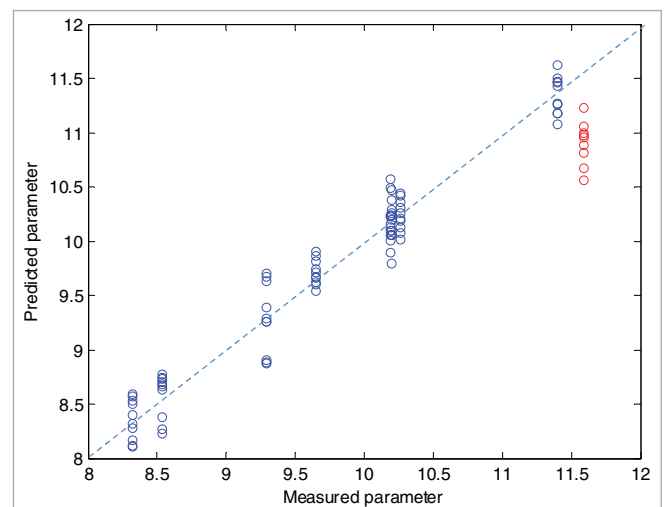


Figure 8. Humidity estimation for out-of-training set bone Batch #3.

Table 4. Average percentile error per test batch.

	Batch #1	Batch #2	Batch #3	Batch #4	Batch #5	Batch #6	Batch #7	Batch #8	Batch #9
Humidity	0.64%	3.71%	5.93%	13.11%	22.19%	53.48%	22.2%	6.02%	1.74%
Fat	57%	68%	125%	1.31%	165%	27.1%	188%	52%	10.8%
Protein	9.3%	8.1%	5.44%	10.8%	13.18%	11.7%	17.5%	6.6%	5.4%
Mineral	1.1%	3.2%	11.8%	8.6%	28.9%	3.01%	8.8%	9.6%	3.6%

Only the fat prediction on test batches has high errors. This could be explained by the fact that fat has the lowest percentile parameter (between 2% and 3%). We already explained in Table 1 that the sum of all components should be 100%, however, it oscillates between 98% and 101%. This indicates that the error in the chemical measurements could potentially be higher in the fat measurement, having a negative impact on the model training as well as on testing of new batches.

## Conclusions

In conclusion, the Vis-NIR spectral response of dehydrated bones, when including all bone batches available in the training, is a promising and robust metric that correlates well with the measured values of humidity, protein, fat and mineral content. When leaving out any individual batch for testing, the prediction accuracy lowers but it is still acceptable for humidity, protein and mineral. In order to build a more robust model, validation with a wider set of bone batches would be beneficial since the bone batches available are very heterogeneous within and in between batches. In addition, providing a more accurate chemical ground truth could also help further increasing the model robustness, in particular in the case of fat estimation.

Finally, we would like to extend this work to portable and compact hyperspectral cameras such as the Imec Ximea Mosaic camera<sup>7</sup> offering 25 bands in the same Vis-NIR range. Its small form factor and portability would enable applications for on-site quick inspection of the mentioned chemical parameters.

## References

1. H-J. He, D. Wu and D-W. Sun, "Application of hyperspectral imaging technique for non-destructive pH prediction in salmon fillets", *The 3rd CIGR International Conference of Agricultural Engineering (CIGR-AgEng2012)*, Valencia, Spain (2012).
2. S. Kazemi, M. Ngadi, N. Wang and S.O. Prasher, "The use of VIS/NIR hyper-spectral analysis on moisture and fat content predictions for breaded-fried chicken nuggets", *Asian Journal of Information Technology* **5**, 1343–1350 (2006). <http://bit.ly/2eV66TK>
3. D. Vincke, D. Eylembosch, J.A. Fernández Pierna, V. Baeten, B. Bodson and P. Dardenne, *Analysis of Collagen Preservation in Bones Recovered in Archaeological Contexts using NIR Hyperspectral Imaging*. WHISPERS (2014).
4. K. Tack, A. Lambrechts, P. Soussan and L. Haspeslagh, "A compact, high-speed and low-cost hyperspectral imager", *Proc of SPIE* **8266**, 82660Q (2012). doi: <https://doi.org/10.1117/12.908172>
5. S. de Jong, "SIMPLS: an alternative approach to partial least squares regression", *Chemometr. Intell. Lab. Syst.* **18**, 251–263 (1993). [https://doi.org/10.1016/0169-7439\(93\)85002-X](https://doi.org/10.1016/0169-7439(93)85002-X)
6. R. Rosipal and N. Kramer, "Overview and recent advances in partial least squares", in *Subspace, Latent Structure and Feature Selection*, Ed by C. Saunders, M. Grobelnik, S. Gunn and J. Shawe-Taylor. Lecture Notes in Computer Science Vol. 3940, Springer, Berlin, Heidelberg, pp. 34–51 (2006). [https://doi.org/10.1007/11752790\\_2](https://doi.org/10.1007/11752790_2)
7. B. Geelen, N. Tack and A. Lambrechts, "A compact snapshot multispectral imager with a monolithically integrated per-pixel filter mosaic", *Proc. SPIE* **8974**, 89740L (2014). doi: <https://doi.org/10.1117/12.2037607>